

Experiment and modeling study on the multiphase reactive transport under supercritical geothermal conditions

Tianfu Xu, Chenghao Zhong, Guanhong Feng, Yilong Yuan, and Ye Gong

Key Laboratory of Groundwater Resources and Environment, Ministry of Education, Jilin University, Changchun, 130021, China

Tianfu_Xu@jlu.edu.cn

Keywords: Supercritical geothermal, experiment, modeling, multi-phase flow, reactive transport

ABSTRACT

Supercritical geothermal (SG) resources are renewable and carbon-free energy resources with enormous potential. The equilibrium and reaction kinetics parameters of quartz fluctuate within sub- to supercritical geothermal conditions (300-500°C), which makes the distribution of formation porosity and permeability difficult to predict. In this study, we conducted a series of water-quartz interaction experiments to determine its solubility and dissolution rate constant under the SG conditions. The results indicate that the quartz solubility and dissolution rate constant have a similar fluctuating behavior, under subcritical and supercritical geothermal conditions. Compared with previous studies, our results showed slightly higher solubility near the supercritical point and in low-density areas. This discrepancy can be attributed to the enhanced accuracy achieved through our adopted method of the vacuum in-situ sampling and rapid on-site testing, which can result in higher accuracy. Based on our results and previously available data, we proposed a novel prediction model for quartz solubility and dissolution rate constants. Using these prediction models, we have developed an innovative reactive transport modeling program that integrates multiphase flow, solute transport, and chemical behavior of quartz across steam/liquid and supercritical phases in various environments. Furthermore, based on the geothermal conditions in the Kakkonda geothermal field, in Japan, a 3-D reservoir exploitation model was constructed by the improved program. We identified the quartz dissolution/precipitation characteristic in the reservoir and its influence mechanism on the sustainable exploitation of SG systems. These findings offer valuable insights into the maximum potential within the Kakkonda area, facilitating a preliminary understanding of the geochemical behavior of quartz in the SG development.

1. INTRODUCTION

The exploitation of supercritical geothermal (SG) resources is a frontier field in geothermal energy. The SG resources have been defined typically as being above the critical temperature and pressure (374°C, 22.1 MPa) of pure water (Michaelides, 1986). Up to now, several geothermal sites around the world have been drilled up to SG conditions, showing SG resources that have the potential to provide a near-unlimited source of renewable energy (Cladouhos et al., 2018).

As the second abundant silicate mineral, quartz interacts significantly with SG fluids, when fluids circulate in reservoirs. The dissolution/precipitation of quartz may significantly affect the hydraulic and mechanical properties of the rock media, especially in its porosity and permeability (Watanabe et al., 2020). However, the equilibrium and kinetic parameters of quartz are incomplete within sub- to supercritical geothermal conditions (300-500°C), making the distribution of formation porosity and permeability difficult to predict (Zhong et al., 2024). In addition, there is no unified model to accurately reproduce the thermodynamic and kinetic parameters of quartz up to supercritical conditions, which restricted the application of SG Thermal-Hydraulic-Chemical (THC) coupled simulation programs (Feng et al., 2022). As a consequence, it is impossible to carry out quantitative evaluations of relevant deep hydrogeochemical processes.

In this study, using the improved experimental system and sampling method, we carried out a series of quartz dissolution thermodynamic and reaction kinetic experiments to investigate the solubility and dissolution rate constants of quartz at 300-500°C and 25-50 MPa. Using our results and previously available data, we proposed a novel prediction model for quartz solubility and kinetic rate constants, then developed an innovative reactive transport modeling program. Furthermore, based on the geothermal conditions in the Kakkonda geothermal field, in Japan, a 3-D reservoir exploitation model was constructed by the improved program. We identified the quartz dissolution/precipitation characteristic in the reservoir and its influence mechanism on the sustainable exploitation of SG systems. The results presented in this work provide scientific theories and experimental data support for solving problems related to deep fluid geoscience issues and SG development projects.

2. METHODS

2.1 Quartz-water interaction

Aqueous silica exists as a neutral hydrated monomer species H_4SiO_4 in pure water (Helgeson, 1969). Thus, the quartz-water reaction can be expressed as follows:



Based on the law of mass action, Equation (1) is written as:

$$\log m_{\text{H}_4\text{SiO}_4(\text{aq})} = \log K \quad (2)$$

where K is the equilibrium constant and $m_{\text{H}_4\text{SiO}_4(\text{aq})}$ is the molality of aqueous silica. According to the equation, the quartz solubility obtained through the chemical analysis of a solution is its thermodynamic equilibrium constant.

A first-order rate equation is used to describe the dissolution process of quartz (Rimstidt and Barnes, 1980), as follows:

$$r = k \left(\frac{A}{M} \right) (a_{\text{SiO}_2}) (a_{\text{H}_2\text{O}})^2 \left(1 - \frac{m}{m_{\text{sat}}} \right) \quad (3)$$

where r is the reaction rate (mol/m²/s), k is the rate constant (mol/m²/s), M is the relative mass of water in the system, normalized to one kilogram (kg), A is the relative interfacial area, normalized to one square meter (m²), a_{SiO_2} and $a_{\text{H}_2\text{O}}$ are the activity of silica and water, respectively.

Based on the concentration vs. time curve obtained by a series of batch reaction kinetic experiments, the rate constant of quartz dissolution is calculated from the following integral form of Equation (3), as follows:

$$k = -\ln \left(\frac{m_{\text{sat}} - m_{t+\Delta t}}{m_{\text{sat}} - m_t} \right) \left(\frac{M}{A} \right) \frac{m_{\text{sat}}}{\Delta t} \quad (4)$$

where t is the time (s). In this study, the specific surface area of mineral particles is estimated by the B.E.T. (Brunauer-Emmett-Teller) method (Brunauer et al., 1938). The water mass in the reactor is estimated from the experimental values of temperature, pressure, vessel volume, and water density (Wagner et al., 2000).

2.2 Experimental sample

The quartz samples used in our experiments were collected from a quartz-vein-type gold deposit in Hebei province, China. The silica content of the samples reached a high purity level. These samples were crushed in a steel mortar and sieved to obtain the 1 to 3 mm mesh fraction. Before the experiment, we washed the sample surface with ultrapure water to remove impurities.

2.3 Experimental system

A custom-designed experiment system has been constructed to allow conducted rock-fluid interaction experiments up to 550°C and 55 MPa, as shown in Figure 1. The system includes four main parts: reactor apparatus, resistance monitoring apparatus, temperature control system, and pressure control system. As shown in Figure 1, the reactor with a volume of 1L consists of alloy steel. The reactor is heated by a furnace controlled by a temperature regulator and is wrapped with lagging to reduce heat loss. The reactor top cover is provided with a thermowell and pressure gauge to feedback on inside conditions, and a sampling tube for sampling or draining. The reactor is filled with water at the beginning to avoid the gas effects. Therefore, the system pressure is controlled by appropriately draining the fluid using the sampling tube, during the heating process. Furthermore, the change in solution resistance is recorded in real time by the connection between the electrode, resistance tester, and display terminal, which provides a reference for the reaction extent.

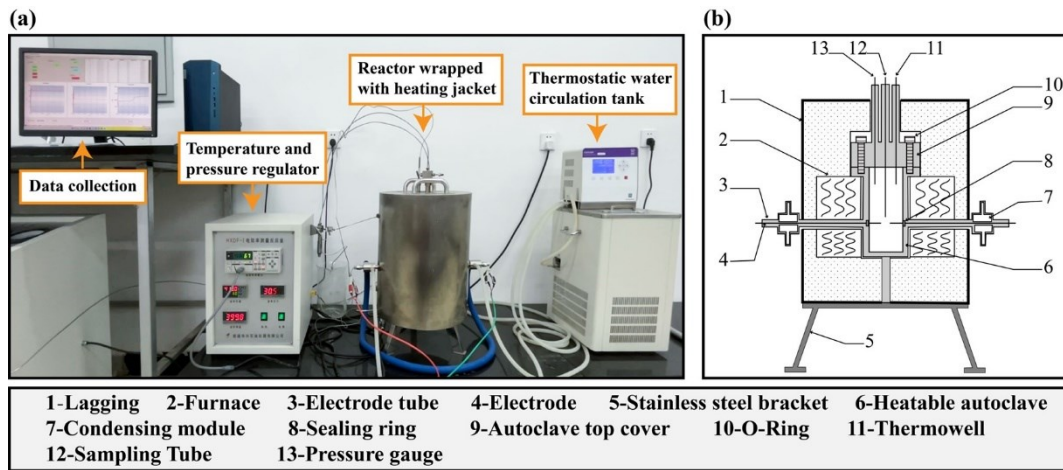


Figure 1: (a) Experiment system and (b) schematic of the reactor for the quartz dissolution experiment.

To obtain solution samples under in-situ temperature and pressure conditions, we employed an in-situ vacuum sampling device with a volume of 10 mL, as shown in Figure 2. Before the sampling, the sampling device is vacuumed and preheated. Then, the sampling device

is connected to the sampling tube to quickly complete the sampling. The extracted solution is diluted (50:1) immediately to minimize precipitation effects, 20 ml of which is used for the analysis of monomeric silica, by the silicomolybdc acid spectrophotometric method.



Figure 2: In-situ sampling method.

2.4 Experimental scheme

In thermodynamic experiments of quartz dissolution, 54 runs of solubility measurement were conducted at the temperature from subcritical (300-374°C) to supercritical (374-500°C) and the pressure from 25 to 50 MPa. In reaction kinetic experiments of quartz dissolution, 24 runs of the batch experiment (each run including at least five solubility measurements) were conducted at the same temperature and pressure range as the thermodynamic experiments.

2.5 Reactive transport modeling method

TOUGH2 is a general-purpose numerical simulation program for non-isothermal flows of multi-component, multiphase fluids in porous and fractured media (Pruess 1991, Pruess et al., 1999). Different equation-of-state (EOS) modules are developed for application in different geological scenarios, such as geothermal, CO₂ sequestration, etc. TOUGHREACT (Xu et al., 2006, Xu et al., 2011a, b) is developed based on TOUGH2 with the extension of reactive transport modeling. The code has been applied to study extensively subsurface thermo-physical and geochemical processes. It can describe the interactions between minerals and fluids under local equilibrium or kinetic conditions, with coupling to solute transport in non-isothermal multiphase multi-component flow. The accuracy of this code has been well verified by substantial studies in different domains around the world.

In this study, we have developed an EOS module that can handle the supercritical conditions following Croucher and O'Sullivan (2008), Magnusdottir and Finsterle (2015), incorporating IAPWS-IF97 to calculate the physical and chemical properties of water under different phase conditions (Feng et al., 2021, Feng et al., 2022). The upper limits for pressure and temperature of IAPWS-IF97 are 100 MPa and 800°C, and when the pressure is below 50 MPa the temperature could reach up to 2000 °C.

In TOUGH2, the items for the mass conservation equation are calculated by each phase and then assemble the matrix together. For supercritical conditions, the phases involve liquid (water), gas (steam), and supercritical phase. The phase boundary between water and steam is the saturation line, while, there is no boundary between water/supercritical and steam/supercritical. In this study, we propose to extend the saturation line, and artificially divide the supercritical phase into two parts, supercritical “gas” and supercritical “liquid” (Feng et al., 2021, Feng et al., 2022). The iso-density contour line of critical density (322 kg/m³) in the supercritical conditions is selected as the virtual extended saturation line. Thus, the system involving supercritical conditions could be treated as a regular liquid/gas two-phase system.

Based on experimental results, we incorporate the density-based models of quartz solubility and dissolution rate constant to extend the chemical database of the TOUGHREACT simulator up to the SG conditions. Even if the data is obtained, within the current reactive transport modeling framework, the solute transport of primary species and chemical reactions are constrained in aqueous phases, and the pertinent geochemical behavior in steam and supercritical phases is neglected. In this study, a weighting method is proposed to describe geochemical reactions in both the steam, aqueous, and supercritical phases, which is introduced in Feng et al. (2022). The improved reactive transport modeling program integrates multiphase flow, solute transport, and chemical behavior of quartz across steam/liquid and supercritical phases in various environments.

3. EXPERIMENTAL RESULTS

3.1 Thermodynamic experiment

The quartz solubilities in water determined by 54 in-situ measurements are shown in Figure 3. The results indicate that the quartz solubility in water is significantly affected by pressure above 300°C and has a positive correlation with pressure at a constant temperature. With increasing temperature, the quartz solubility increases in the subcritical region and then decreases near the supercritical region. This phenomenon, known as the retrograde behavior of quartz solubility, becomes more pronounced at low pressures. However, the retrograde behavior gradually disappears at higher temperatures and pressures.

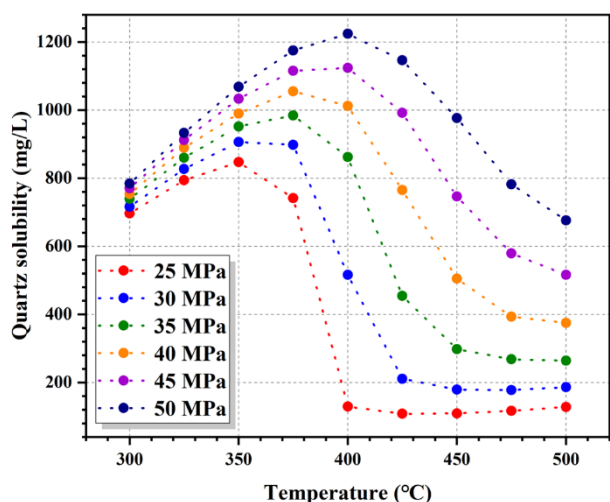


Figure 3: Quartz solubilities as a function of temperatures along isobaric conditions.

The experiments under the same temperature and pressure as in this study are selected to compare the difference in quartz solubility with previous measurements, as shown in Figure 4. The results indicate that the quartz solubilities measured in this study are significantly greater than those of Kennedy (1950) near the supercritical point, and somewhat greater than those of Rendel and Mountain (2023) under the low-density condition. The lower experiment results of Kennedy (1950) may be caused by 1) the experiments having insufficient time to attain equilibrium, and 2) the polymerization and precipitation of silica when using the rapid-quench method. Furthermore, the lower experiment results of Rendel and Mountain (2023) may be caused by silica precipitates when vaporous water condenses into a liquid during sampling. In this study, we employed the in-situ sampling method (Figure 2) to fill these deficiencies as far as possible.

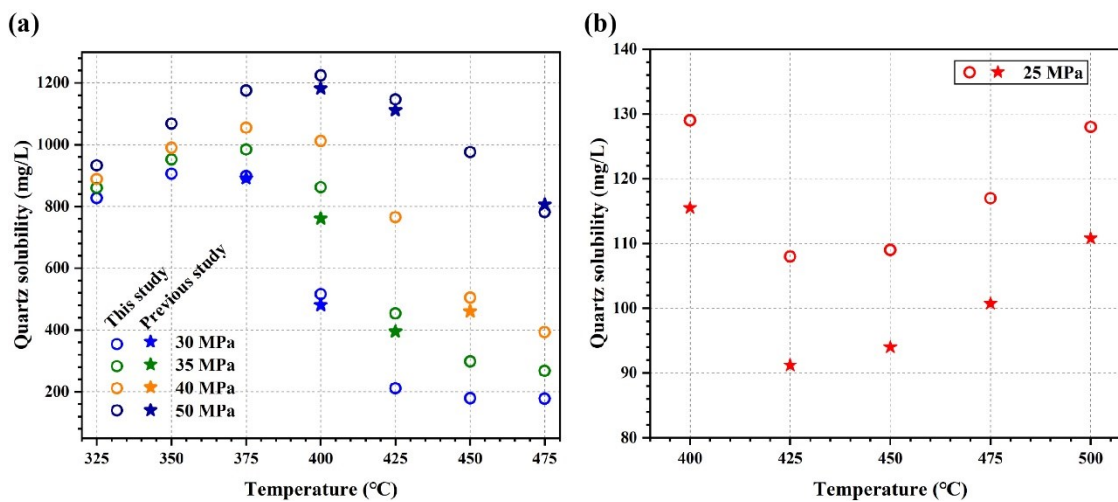


Figure 4: Differences in the measured quartz solubility between this study and (a) Kennedy (1950) and (b) Rendel and Mountain (2023).

3.2 Reaction kinetic experiment

Based on the 24 runs of batch experiments, the dissolution rate constants of quartz in water were obtained, as shown in Figure 5. Noteworthy, the quartz dissolution rate constant has a similar fluctuating behavior to its solubility, under subcritical and supercritical geothermal conditions. At a constant temperature, there exists a positive correlation with pressure. At a constant pressure, the rate constant increases with increasing temperature in the subcritical region and then decreases with further increasing temperature when entering the supercritical region. This fluctuating feature has been already documented in the literature (Tsuchiya and Hirano, 2007; Zhang et al., 2015).

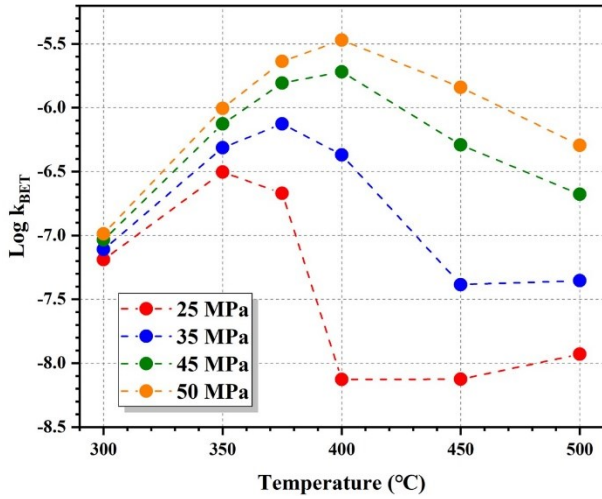


Figure 5: Rate constants based on the BET method as a function of temperatures along isobaric conditions.

At subcritical and supercritical regions, the experiment results suggest that the rate constant departs the main trend due to the significant pressure effect. Therefore, it is necessary to consider the pressure effect to evaluate the quartz dissolution rate under subcritical and supercritical conditions. Zhang et al. (2015), Dove and Crerar (1990), and Dove (1999) measured the quartz dissolution rate in water from 11 MPa to 33 MPa using a continuous stirred-tank reactor, as shown in Figure 6. These results of individual experiments indicate that pressure has a positive effect on the quartz dissolution rate. However, the results of Zhang et al. (2015) at 23 MPa and 33 MPa are significantly higher than others, possibly because of a memory effect due to pretreatment with acetone done to remove fine particles from quartz particles. At the same temperature of 300°C, our results at high pressure are lower than those of Dove and Crerar (1990) at low pressure. One possible explanation for this discrepancy is the different behavior of closed experimental systems, which are characterized by a lower concentration limit, compared to the open systems of Dove and Crerar (1990).

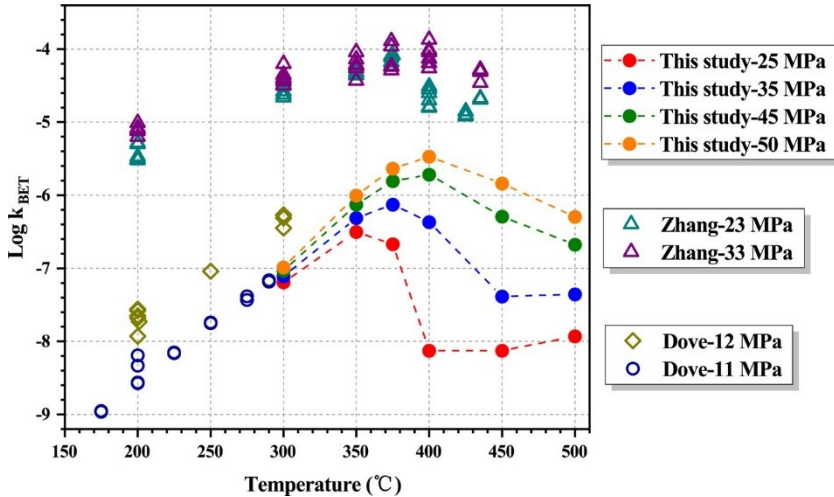


Figure 6: Rate constants as a function of temperatures along isobaric conditions.

3.3 Empirical density models for quartz solubility and dissolution rate constant

Up to now, several empirical models have been suggested for calculating the quartz solubility in water over a wide range of temperature and pressure conditions (Dolejš, 2013). These models were fitted on calibration to experimental data, and their applicability was strictly limited to the experimental range. The extrapolation outside these limits has proved to be critical, because of incorrect results. Any improvement of the existing solubility models for quartz requires the collection of new accurate data on quartz solubility in water. Based on our results, we employed the five-parameter equation of the density model by Dolejš and Manning (2010) for regression analysis, as follows:

$$\ln m = -\frac{1}{R} \left(\frac{a}{T} + b + c \ln T + dT + e \ln \rho_{\text{H}_2\text{O}} \right) \quad (5)$$

where m is the molal silica concentration; T is the absolute temperature; R is the universal gas constant $8.314 \text{ J}/(\text{mol}\cdot\text{K})$; ρ is the solution density in g/cm^3 ; a to e are mineral-specific thermodynamic coefficients.

The parameterization a to e of Equation (5) was achieved by combining our measurements and the selected previous results (Zhong et al., 2024). The IAPWS-IF97 formulation (Wagner et al., 2000) was used to associate appropriate temperature, pressure, and density values to each experimental determination. In order to discard anomalous data, experimental data below 300°C were scrutinized with respect to Rimstidt (1997). At the end of this procedure, the best-fitting relationship was finally obtained, as follows:

$$\ln m = -\frac{1}{R} \left(\frac{20612.36434}{T} - 39.61695 + 9.66155 \ln T - 0.04348T - 14.2389 \ln \rho_{\text{H}_2\text{O}} \right) \quad (6)$$

Up to now, there are not yet generally accepted kinetic models suitable for the prediction of the dissolution rate constant at SG conditions. Herein, we developed an empirical parametric model to characterize the reaction kinetic behavior of quartz dissolution. The law of detailed balancing (Lasaga, 1995) indicates that the dissolution rate constant (k_+) is equal to the equilibrium constant (K) times the precipitation rate constant (k_-), as follows:

$$k_+ = Kk_- \quad (7)$$

and

$$\ln k_+ = \ln K + \ln k_- \quad (8)$$

Thus, similar to the empirical density model used to quantify the quartz solubility (Equation 5), a five-parameter density-based model was developed to describe the quartz dissolution kinetics, as follows:

$$\ln k_+ = -\frac{1}{R} \left(\frac{118168.62}{T} - 1123.92 + 190.42 \ln T - 0.29587T - 36.58 \ln \rho_{\text{H}_2\text{O}} \right) \quad (9)$$

Figure 7 shows the solubility and rate constant of quartz dissolution calculated according to Equations (6) and (9). The results indicate that the predicted results by the density-based models are in great agreement with the experimental dataset (e.g., data from this work and the literature).

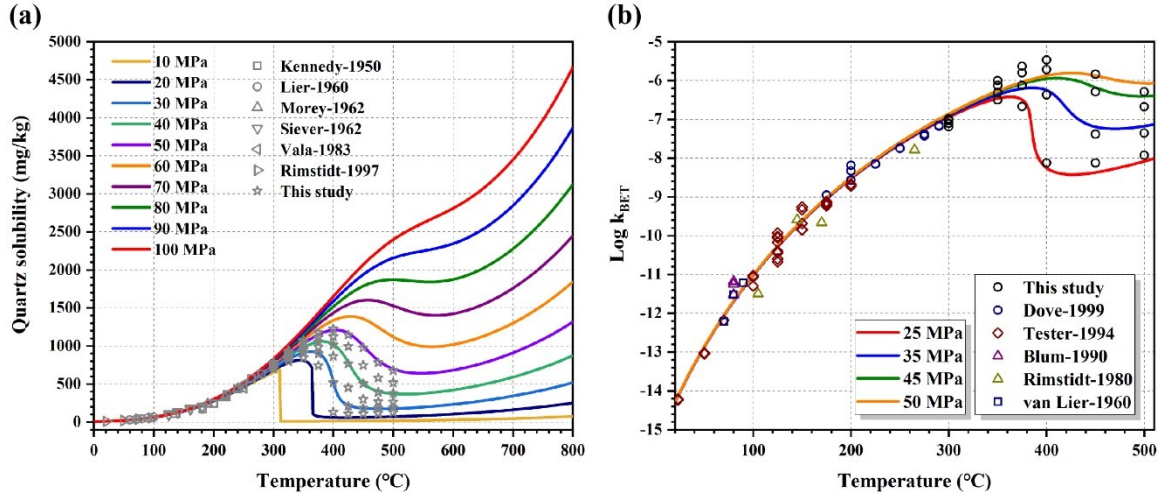


Figure 7: The (a) solubility and (b) rate constants of quartz dissolution calculated from the density-based model.

4. NUMERICAL MODEL APPLICATION

4.1 Geological model

According to the numerical studies of Watanabe et al. (2022), a reconstruction area with a radius of about 150 m can be formed around the injection well by hydraulic fracturing at the SG conditions. Thus, the geometry of the fractured reservoir is assumed to be $(x, y, z) 600 \text{ m} \times 300 \text{ m} \times 300 \text{ m}$, as shown in Figure 8a. In addition, to accurately simulate the heat transfer between the fractured reservoir and the surrounding rock matrix, the simulated area is extended outward by 500 m. Thus, the model geometry is $(x, y, z) 1600 \text{ m} \times 1300 \text{ m} \times 1300 \text{ m}$, as shown in Figure 8b. The depth of the target geothermal reservoir is 2929-4229 m, and the depth of the fractured reservoir is 3429-3729 m. Injection and production wells are located in the middle of the fractured reservoir, both are 300 m apart, and the perforation interval of both is 40 m.

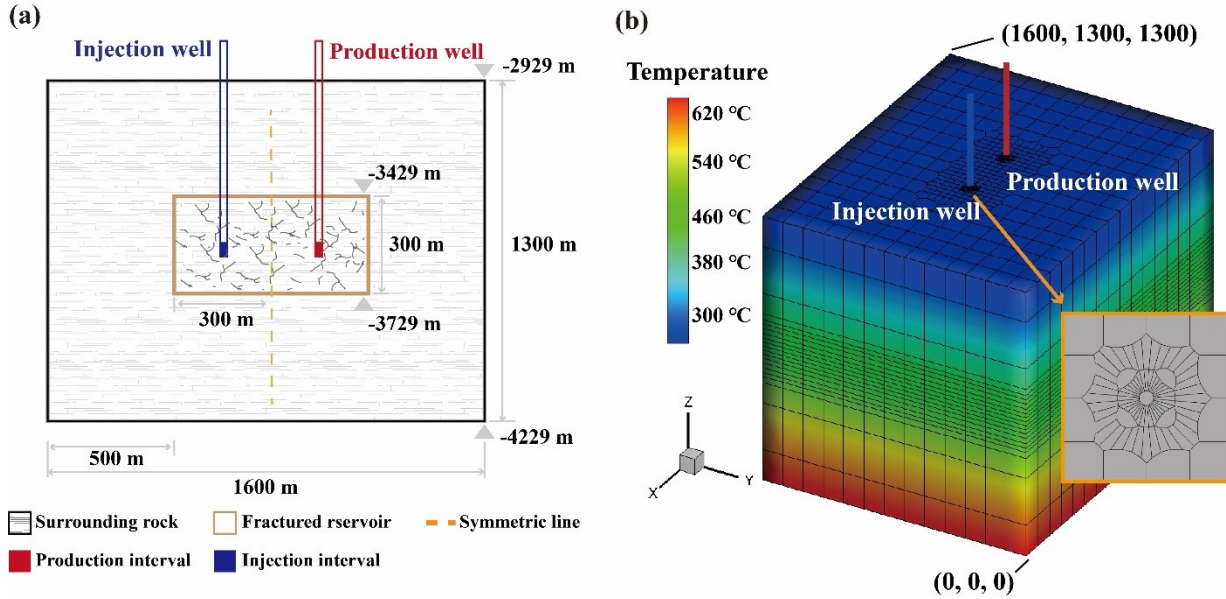


Figure 8: Schematic diagram of (a) the fractured reservoir model and (b) the 3D numerical model.

In the model, we employed the equivalent porous medium method to characterize the fluid flow and heat transfer in the reservoir. According to the geothermal conditions of the WD-1a well, the temperature gradient at the depth of 2929-4229 m is 32 °C/100 m (Ikeuchi et al., 1998). Therefore, the initial temperatures at the top and bottom of the model are 249°C and 665°C, respectively. The initial pressure of the model is about 29 MPa at the top and follows a hydrostatic pressure gradient. To maintain the stability of reservoir pressure, we employed a compensatory production scheme, with an injection flow of 19 kg/s and a production flow of 15 kg/s. The injection temperature is considered to be 60°C.

The exploitation time of this SG system is considered for 20 years. According to the studies of Doi et al. (1998) and Fujimoto et al. (2000), the rock density, specific heat, and thermal conductivity in the model are set as 2700 kg/m³, 980 J/(kg·°C) and 3 W/(m·°C), respectively. The horizontal and vertical permeability of the fractured reservoir and matrix are consistent, which are set as 20×10^{-15} m² and 1×10^{-18} m², respectively. The porosity of the fractured reservoir and matrix is set as 0.1 and 0.01, respectively.

Because quartz is the main mineral in the Kakkonda granite (Doi et al., 1998), we mainly considered the dissolution and precipitation processes of quartz in the model. The initial volume fraction of quartz is set as 45%. In the model, quartz dissolution/precipitation is considered to be controlled by reaction kinetics, which is related to the kinetic rate constant and reaction surface area. The reaction surface area of quartz is estimated to be 98 cm²/g. Furthermore, we considered pure water as the working fluid. The initial hydrochemistry component in the reservoir is the equilibrium concentration of quartz under reservoir temperature and pressure conditions.

4.2 Simulation results and discussion

Figures (9) and (10) show the temporal and spatial distribution of quartz volume fraction and permeability in the fractured reservoir, during the 20 years of production, respectively. Because the injection fluid is pure water, the quartz around the injection well is dissolution at the initial stage of production (Figure 9a). In the stable stage of production (1-5 years), the low-temperature fluid around the injection well expands and the silica concentration in the fluid does not reach saturation, leading to the further expansion of the quartz dissolution area (Figures 9a-b). Correspondingly, the rock permeability around the injection well significantly increased (Figures 10a-b). In the declining stage of production (5-20 years), the unsaturated fluid extends from the bottom of the fissure reservoir to the production well. Correspondingly, the quartz dissolution area (Figures 9c-d) and the permeability increase area (Figures 10c-d) are basically consistent. Furthermore, it is worth noting that a high permeability zone is formed above the perforating section of the injection well (Figure 9d). This phenomenon may be due to the retrograde dissolution behavior of quartz near the supercritical point (Figure 7). The formation of local high permeability zones around injection wells is conducive to the efficient recharge of geothermal tailwater. During the 20 years of production, quartz continuously precipitates around the production well (Figures 9a-d). This leads to a significant reduction of rock permeability around the production well (Figures 10a-d). The simulation results indicate that the volume fraction of quartz in the perforating section of the production well increases by 52.31% caused by quartz precipitation, and the rock permeability decreases about one order of magnitude from the initial 20 mD to 2.98 mD, during the 20 years of production. The quartz precipitation problem near the production well has a great impact on the sustainable exploitation of SG systems.

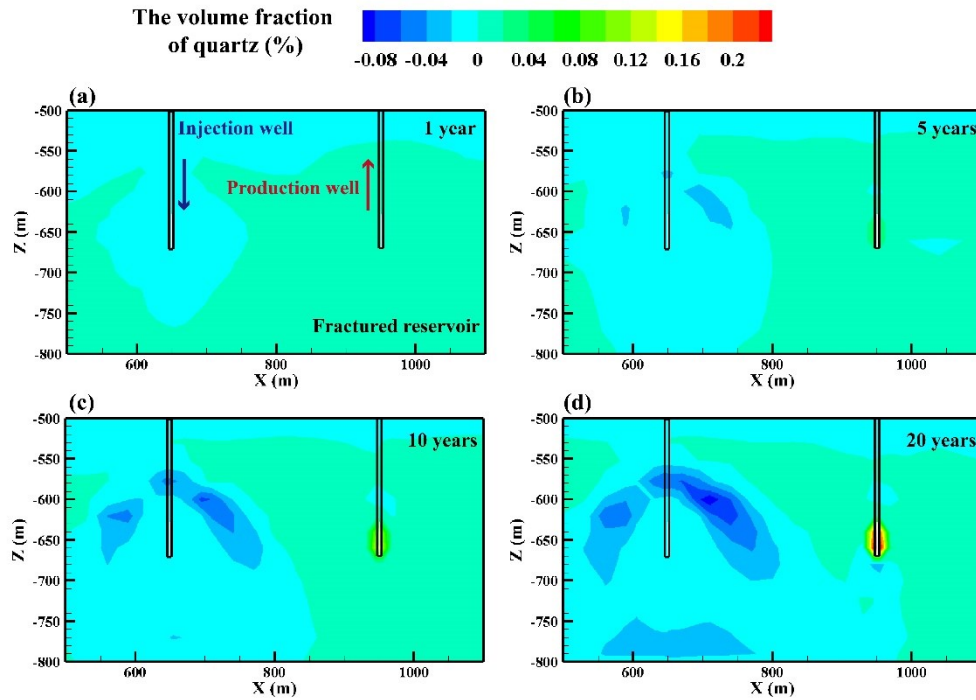


Figure 9: The spatial and temporal distribution of quartz volume fraction in fractured reservoirs at (a) 1 year, (b) 5 years, (c) 10 years, and (d) 20 years during the production of SG systems.

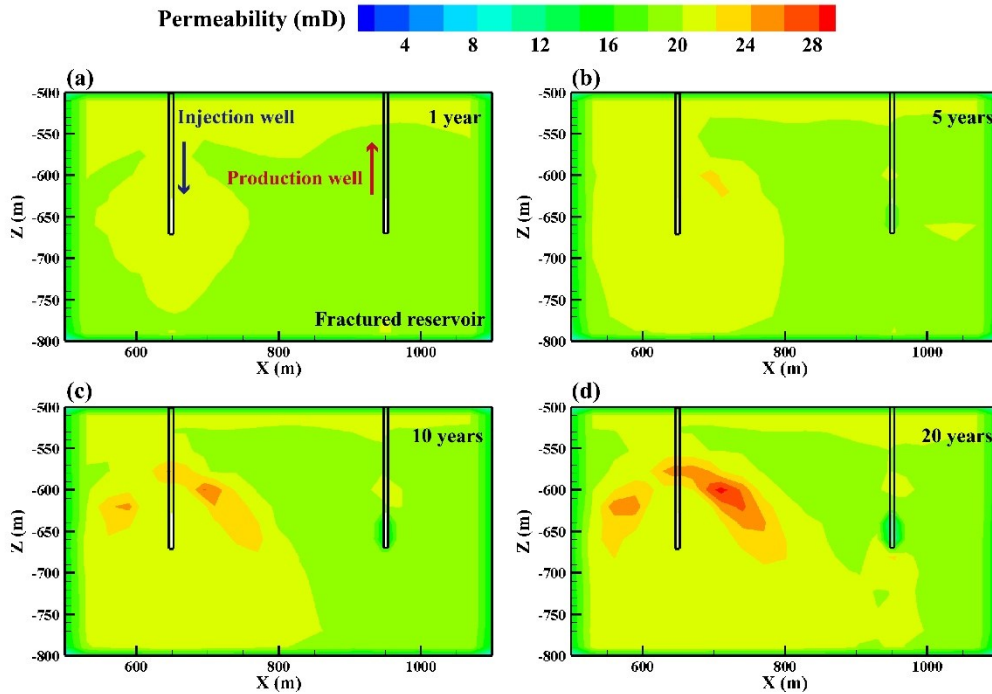


Figure 10: The spatial and temporal distribution of permeability in fractured reservoirs at (a) 1 year, (b) 5 years, (c) 10 years, and (d) 20 years during the production of SG systems.

5. CONCLUSION

The quartz dissolution/precipitation plays an important role in the formation, migration, accumulation, and exploitation of SG fluids. In this study, we carried out a series of thermodynamic and reaction kinetic experiments of quartz dissolution, at the temperature from subcritical (300-374°C) to supercritical (374-500°C) and the pressure from 25 MPa to 50 MPa. The experiment results indicate that the

quartz solubility and dissolution rate constant have a similar fluctuating behavior from sub- to supercritical geothermal conditions. Under constant pressure conditions, the quartz solubility and dissolution rate constant increase with the increasing temperature in the subcritical region, then decrease with the increasing temperature in the supercritical region. Under constant temperature conditions, the quartz solubility and dissolution rate constant are positively correlated with the pressure. Furthermore, our results are combined with previously available data to develop quartz dissolution thermodynamic and kinetic density models. These models can be used to quantitatively calculate the dissolution concentration of silica and the reaction rate in geothermal fluids from normal to SG conditions. Based on these models, we developed an innovative reactive transport modeling program that integrates multiphase flow, solute transport, and chemical behavior of quartz across steam/liquid and supercritical phases in various environments. Furthermore, using the improved program, we established a 3D exploitation model of an SG reservoir to analyze the evolution characteristics of reservoir permeability at long-term geothermal production. The simulation results indicate that, during the long-term heat recovery, a high permeability zone forms above the perforating section of the injection well due to the retrograde behavior of quartz dissolution, which is conducive to the efficient recharge of the geothermal tailwater. However, due to the obvious depressurization of the rock layer near the perforation section of the production well, serious silica precipitation problems and formation permeability decrease (about one order of magnitude), which have a great impact on the sustainable exploitation of SG. These findings offer valuable insights into the maximum potential within the Kakkonda area, facilitating a preliminary understanding of the geochemical behavior of quartz in SG development.

REFERENCES

- Brunauer, S., Emmett, P.H., and Teller, E.: Adsorption of Gases in Multimolecular Layers, *Journal of the American Chemical Society*, 60, (1938), 309-319.
- Cladouhos, T., Petty, S., Bonneville, A.H., Schultz, A., and Sørli, C.F.: SuperHot EGS and the Newberry Deep Drilling Project, p. Medium: X, Pacific Northwest National Lab (PNNL), Richland, WA (United States), United States (2018).
- Croucher, A., O' Sullivan, M.: Application of the Computer Code TOUGH2 to the Simulation of Supercritical Conditions in Geothermal Systems, *Geothermics*, 37, (2008), 622-634
- Doi, N., Kato, O., Ikeuchi, K., Komatsu, R., Miyazaki, S., Akaku, K. and Uchida, T.: Genesis of the plutonic-hydrothermal system around quaternary granite in the kakkonda geothermal system, Japan, *Geothermics*, 27, (1998), 663-690.
- Dolejš, D.: Thermodynamics of Aqueous Species at High Temperatures and Pressures: Equations of State and Transport Theory, *Reviews in Mineralogy and Geochemistry*, 76, (2013), 35-79.
- Dolejš, D., and Manning, C.E.: Thermodynamic model for mineral solubility in aqueous fluids: theory, calibration and application to model fluid-flow systems, *Geofluids*, 10, (2010), 20-40.
- Dove, P.M.: The dissolution kinetics of quartz in aqueous mixed cation solutions, *Geochimica et Cosmochimica Acta*, 63, (1999), 3715-3727.
- Dove, P.M., and Crerar, D.A.: Kinetics of quartz dissolution in electrolyte solutions using a hydrothermal mixed flow reactor, *Geochimica et Cosmochimica Acta*, 54(4), (1990), 955-969.
- Feng, G., Wang, Y., Xu, T., Wang, F., and Shi, Y.: Multiphase Flow Modeling and Energy Extraction Performance for Supercritical Geothermal Systems, *Renewable Energy*, 173, (2021), 442-454.
- Feng, G., Xu, T., Zhao, Y., and Gherardi, F.: Heat Mining From Super-hot Horizons of the Larderello Geothermal Field, Italy. *Renewable Energy* 197, (2022), 371-383.
- Fujimoto, K., Takahashi, M., Doi, N. and Kato, O. 2000 High permeability of Quaternary granites in the Kakkonda geothermal area, northeast Japan (proceedings).
- Helgeson, H.C. 1969. Thermodynamics of hydrothermal systems at elevated temperatures and pressures. *American Journal of Science* 267, 729-804.
- Ikeuchi, K., Doi, N., Sakagawa, Y., Kamenosono, H., and Uchida, T.: High-temperature measurements in well WD-1A and the thermal structure of the kakkonda geothermal system, Japan, *Geothermics*, 27, (1998), 591-607.
- Kennedy, G.C.: A portion of the system silica-water, *Economic Geology*, 45, (1950), 629-653.
- Lasaga, A.C.: Fundamental approaches in describing mineral dissolution and precipitation rates, *Reviews in Mineralogy and Geochemistry*, 31, (1995), 23-86.
- Magnusdottir, L., and Finsterle, S.: An iTOUGH2 Equation-of-state Module for Modeling Supercritical Conditions in Geothermal Reservoirs, *Geothermics*, 57, (2015), 8-17,
- Michaelides, E.E.: NBS/NRC Steam Tables: Thermodynamic and Transport Properties and Computer Program for Vapor and Liquid States of Water in SI Units, *Nuclear Technology*, 75, (1986), 232-232.
- Pruess, K., TOUGH2: A General-purpose Numerical Simulator for Multiphase Fluid and Heat flow, Lawrence Berkeley Lab. Berkeley, Calif. (1991)
- Pruess, K., Oldenburg, C., and Moridis, G.: TOUGH2 User's Guide, Version 2.0, Report LBNL-43134, Lawrence Berkeley National Laboratory, Berkeley, Calif. (1999)

Xu et al.

- Rendel, P.M., and Mountain, B.W.: Solubility of quartz in supercritical water from 375 °C to 600 °C and 200-270 bar, *The Journal of Supercritical Fluids*, 196, (2023), 105883.
- Rimstidt, J.D.: Quartz solubility at low temperatures, *Geochimica et Cosmochimica Acta*, 61, (1997), 2553-2558.
- Rimstidt, J.D., and Barnes, H.L.: The kinetics of silica-water reactions, *Geochimica et Cosmochimica Acta*, 44, (1980), 1683-1699.
- Tsuchiya, N., and Hirano, N.: Chemical reaction diversity of geofluids revealed by hydrothermal experiments under sub- and supercritical states, *Island Arc*, 16, (2007), 6-15.
- Wagner, W., Cooper, J.R., Dittmann, A., Kijima, J., Kretschmar, H.J., Kruse, A., Mares, R., Oguchi, K., Sato, H., Stocker, I., Sifner, O., Takaishi, Y., Tanishita, I., Trubenbach, J., and Willkommen, T.: The IAPWS Industrial Formulation 1997 for the Thermodynamic Properties of Water and Steam, *Journal of Engineering for Gas Turbines and Power*, 122, (2000), 150-184.
- Watanabe, K., Watanabe, N., Watanabe, N., Sakaguchi, K., Aichi, M., Ouchi, H., and Asanuma, H.: A numerical study on the creation of artificial supercritical geothermal reservoirs by hydraulic fracturing, *Geothermics*, 105, 2022, 102500.
- Watanabe, N., Saito, K., Okamoto, A., Nakamura, K., Ishibashi, T., Saishu, H., Komai, T., and Tsuchiya, N.: Stabilizing and enhancing permeability for sustainable and profitable energy extraction from superhot geothermal environments, *Applied Energy*, 260, (2020), 114306.
- Xu, T., Sonnenthal, E., Spycher, N., and Pruess, K.: TOUGHREACT - A Simulation Program for Non-isothermal Multiphase Reactive Geochemical Transport in Variably Saturated Geologic Media: Applications to Geothermal Injectivity and CO₂ geological Sequestration, *Computers & Geosciences* 32, (2006), 145-165.
- Xu, T., Spycher, N., Sonnenthal, E., Zhang, G., Zheng, L., and Pruess, K.: TOUGHREACT Version 2.0: A Simulator for Subsurface Reactive Transport under Non-isothermal Multiphase Flow Conditions, *Computers & Geosciences* 37, (2011), 763-774.
- Xu, T., Spycher, N., Sonnenthal, E., Zheng, L., and Pruess, K.: TOUGHREACT User's Guide: A Simulation Program for Non-isothermal Multiphase Reactive Geochemical Transport in Variably Saturated Geologic Media, Version 2.0, Report LBNL-DRAFT, Lawrence Berkeley National Laboratory, Berkeley, Calif. (2012)
- Zhang, R., Zhang, X., and Hu, S.: Dissolution kinetics of quartz in water at high temperatures across the critical state of water, *The Journal of Supercritical Fluids*, 100, (2015), 58-69.
- Zhong, C., Xu, T., Yuan, Y., Gherardi, F., and Feng, G.: An experimental study on quartz solubility in water under supercritical geothermal conditions, *Journal of Hydrology*, 630, (2024), 130663.